

Vortex Motion and Vortex Friction Coefficient in Triangular Josephson Junction Arrays

Wenbin Yu and D. Stroud

Department of Physics, The Ohio State University, Columbus, OH 43210

(October 29, 2018)

We study the dynamical response of triangular Josephson junction arrays, modelled as a network of resistively- and capacitively-shunted junctions (RCSJ's). A flux flow regime is found to extend between a lower vortex-depinning current and a higher critical current, in agreement with previous calculations for square arrays. The upper current corresponds either to row-switching events accompanied by steplike jumps in the array resistance, or to a depinning of the entire array. In the flux flow regime, the dynamical response to the bias current is roughly Ohmic, and the time-dependent voltage can be well understood in terms of vortex degrees of freedom. The vortex friction coefficient η depends strongly on the McCumber-Stewart parameter β , and at large β is approximately independent of the shunt resistance R . To account for this, we generalize a model of Geigenmüller *et al* to treat energy loss from moving vortices to the phase analog of optical spin waves in a triangular lattice. The value of η at all values of β agrees quite well with this model in the low-density limit. The vortex depinning current is estimated as $0.042I_c$, independent of the direction of applied current, in agreement with static calculations by Lobb *et al*. A simple argument suggests that quantum effects in vortex motion may become important when the flux flow resistivity is of order $h/(2e)^2$ per unit frustration.

PACS numbers: 74.50.+r, 74.60.Ge, 74.60.Jg, 74.70.Mq

I. INTRODUCTION

The behavior of vortices in Josephson junction arrays (JJA's) has attracted much recent attention.^{1–14} Such vortices are coherent arrangements of phases of the superconducting order parameter, which may move through the array like particles, in response to forces generated by external currents. They can be generated by a magnetic field, or excited thermally. At low velocities, it has been proposed that the motion of a vortex in a square array can be described by a Josephson-like equation of the form³

$$\frac{d^2}{dt^2} \left(2\pi \frac{x}{a} \right) + \frac{1}{RC} \frac{d}{dt} \left(2\pi \frac{x}{a} \right) + \frac{4e}{\hbar C} \left[I_d \sin \left(2\pi \frac{x}{a} \right) - I \right] = 0. \quad (1)$$

Here x is the vortex position along a line through the plaquette centers and perpendicular to the external current I , a is the lattice constant, R and C are the shunt resistance and shunt capacitance of each junction, and I_d is the vortex depinning current, which is linearly related to the junction critical current I_c . This equation may describe the behavior of a vortex in a square array at low velocities.

Because of the mass term in this equation, a vortex might be expected to move ballistically under appropriate circumstances – that is, a vortex, once set into motion, would remain in motion even if the driving current is turned off. There are several experimental reports of such motion^{4,6}. However, numerical calculations and analytical studies, based on *classical* equations of motion, have not yet produced such ballistic motion^{7,9,10,14}. The numerical studies have been carried out either in square arrays^{7,9,14}, or using a simplified representation of the Josephson interaction, in triangular arrays⁷. Instead of ballistic motion, in these simulations, it is generally found that the junctions in the wake of the vortex oscillate, causing the vortex to lose its energy to the array. In an analytical study based on a continuum model¹⁰, an equation of motion for individual vortices is derived for both square and triangular arrays, starting from an effective action for the array. This paper concludes that a narrow window of vortex velocity exists in a triangular array, for which ballistic motion may be possible. However, it seems unlikely that this window is the regime which is probed experimentally^{4,6}.

In this paper, we present dynamical calculations for triangular Josephson junction arrays. The calculations are

carried out within a classical model of resistively- and capacitively-shunted junctions (RCSJ's). Our principal aim is to study the motion of single vortex in the presence of an applied d. c. current, to see if ballistic vortex motion is possible. Since the depth of the vortex potential in a triangular array is believed to be smaller than that of a square array¹⁶, such motion would seem more likely, at first glance, than in square arrays. However, we find no such ballistic motion under any circumstances investigated. Instead, the motion of the vortex, when it is a coherent excitation of the array, generally falls into a “flux flow” regime, where the vortex moves with approximately Ohmic resistivity, described by a characteristic vortex viscosity.

As in previous simulations in square arrays^{7,9,13,14}, and in similar studies in triangular arrays based on a simplified Josephson coupling⁷, we find that the flux flow region terminates at sufficiently high current in either of two ways. One possibility is for the entire lattice of Josephson junctions to be “depinned” causing the voltage to increase sharply. A second decay mode, which predominates in sufficiently underdamped arrays, is for the vortex to excite row switching events, which produce steplike increases of the array resistance as an entire row of junctions switches from superconducting to normal. Both such decay modes have been in a variety of experiments^{5,8,17,18}.

Perhaps the most striking result of our simulations, also reported previously in square arrays^{9,14}, is the persistence of the quasi-ohmic flux-flow regime even in high-resistance arrays where, according to simple models, ballistic motion should be possible. To account for this, we generalize a model of Geigenmüller *et al*⁹ to obtain a simple, nearly analytic model from which an effective vortex friction coefficient can be computed at any value of the vortex velocity and junction McCumber-Stewart coefficient¹⁹

$$\beta = 2eR^2I_cC/\hbar. \quad (2)$$

β is a dimensionless measure of damping in a single junction (large β means low damping). In our generalization, we take explicit account of the array lattice structure, so that a short-wavelength cutoff appears naturally in the resulting expression for the vortex friction coefficient. The model gives semiquantitative agreement with our numerical experiments. In particular, like the continuum model of Ref. 9 for square arrays, it accounts for the persistence of this friction coefficient even at high values

of the shunt resistance R . The present model is, in principle, applicable to dissipation from an arbitrary density of vortices moving with arbitrary velocities, and to losses produced by a. c. external currents. However, we test it here only for single vortex motion.

The remainder of this paper organized as follows. In Section II, we describe our calculational model and numerical method. Section III reports the results of our critical current calculations in triangular arrays both with and without vortices. Section IV describes in greater detail our numerical results in the flux flow regime, and Sections V and VI summarize the vortex friction model, and our investigation of possible ballistic vortex motion. A brief discussion follows in Section VII.

II. MODEL

The relevant geometry of our triangular array is shown in Fig. 1. Within the array interior of the array, each superconducting grain is connected to its six nearest neighbors via Josephson coupling. The boundary conditions involve fixed external current injection. We consider two directions of current injection, as illustrated in the Fig. 1, the so-called $[10\bar{1}]$ direction, and the $[2\bar{1}\bar{1}]$ direction²⁰.

We describe the dynamics within the RCSJ model at zero temperature, as previously described for square arrays^{14,21}. In this model, the current through each junction is the sum of three terms: a charge flow through an effective intergrain capacitance, a current through a shunt resistance, and a Josephson supercurrent. We assume that the supercurrent is sufficiently weak that we can discard the induced screening current.

With these assumptions, the current between grains i and j is:

$$I_{ij} = C_{ij} \frac{d}{dt} V_{ij} + \frac{V_{ij}}{R_{ij}} + I_{c;ij} \sin(\phi_i - \phi_j - A_{ij}). \quad (3)$$

Here I_{ij} is the total current from grain i to grain j ; C_{ij} and R_{ij} are the shunt capacitance and shunt resistance between grain i and grain j ; $I_{c;ij}$ is the critical current of the Josephson junction between grain i and grain j ; ϕ_i is the phase of the order parameter on grain i . V_{ij} and A_{ij} are the voltage difference and magnetic gauge phase factor between grain i and grain j , defined by

$$V_{ij} \equiv V_i - V_j = \frac{\hbar}{2e} \frac{d}{dt} (\phi_i - \phi_j), \quad (4)$$

and

$$A_{ij} = \frac{2\pi}{\Phi_0} \int_{\mathbf{x}_i}^{\mathbf{x}_j} \mathbf{A} \cdot d\mathbf{l},$$

where $\Phi_0 \equiv hc/(2e)$ is the flux quantum, \mathbf{A} is the vector potential of the applied magnetic field and \mathbf{x}_i is the position of the center of grain i . In the present paper, we include only the intergrain capacitance, discarding the capacitance between the grains and ground. Current conservation at each grain is described by Kirchoff's Law,

$$\sum_j I_{ij} = I_{i;ext}, \quad (5)$$

where $I_{i;ext}$ is the external current fed into grain i . We assume that all the capacitances, critical currents, and shunt resistances have unique values C , I_c , and R . Finally, the use of classical equations of motion implies the assumption that quantum effects²² arising from the non-commutativity of charge and phase variables can be neglected.

Our boundary conditions are shown in Fig. 1. In the direction of current injection, we introduce a uniform current $I_{i;ext} = I$ into each boundary grain along one edge, and extract the uniform current from each boundary grain on the other edge. In the transverse direction, we use periodic boundary conditions, as in our previous work¹⁴. The gauge factor A_{ij} satisfies

$$\sum_{\text{plaquette}} A_{ij} = 2\pi \frac{BS}{\Phi_0} = 2\pi f,$$

where B is the magnetic field strength; S is the area of each triangular plaquette; Φ_0 is the flux quantum. f is the so-called frustration. Note that the primitive cell of a triangular array, consists of *two* adjacent triangular plaquettes.

The coupled equations (3), (4) and (5) are solved as described previously¹⁴. We use a fourth-order Runge-Kutta algorithm with time step Δt , where Δt ranges from $0.01t_0$ to $0.05t_0$ ($t_0 = \hbar/(2eRI_c)$ is a characteristic damping time), depending on the desired precision of calculation. Further details may be found in Ref. 14.

III. CRITICAL CURRENT AND VORTEX DEPINNING CURRENT

When $f = 0$, with d. c. bias current injected in the $[10\bar{1}]$ direction, we find a critical current of exactly $2I_c$. This value can be easily understood, since in this case no current passes through the junctions perpendicular to the

bias current, so that the entire array behaves much like a single junction. With $[2\bar{1}\bar{1}]$ current injection, the critical current is found to be approximately $1.76I_c$. This value can be understood by considering the single triangular plaquette shown in Fig. 2. For such an arrangement, the injected current I is related to the phase difference ϕ by $I/I_c = \sin\phi + \sin(2\phi)$. The right hand side cannot exceed $(I/I_c)_{max} = 1.7602$, which corresponds to our numerically obtained array value. We have checked the phase configuration for each grain in the array in this geometry, and find that it decomposes exactly into unit cells of this type.

Next, we discuss the dynamical response of an array under d. c. bias and in the presence of a single vortex. Such a vortex can be introduced by considering an $N \times N$ array containing $2N^2$ triangular plaquettes, and a flux $f = 1/(2N^2)$ (N being the number of junctions spanning the array in one direction, as in Fig. 1). Table 1 lists the critical currents I_d for $f = 1/(2N^2)$ as a function of N for $[10\bar{1}]$ current injection. This critical current appears to be independent of β , at least in the range $0 \leq \beta \leq 1000$. The critical currents are extracted from an $I - \langle V \rangle$ plot, such as shown in Fig. 3 for $[10\bar{1}]$ current injection at $\beta = 0$ and $\beta = 10$, and Fig. 4 for $[2\bar{1}\bar{1}]$ direction at $\beta = 0$. Extrapolating by eye a plot of I_d versus $1/N$ towards $N = \infty$ at $f = 1/(2N^2)$, we estimate a critical current of about $0.042I_c$ for bias current injected in the $[10\bar{1}]$ direction. In the $[2\bar{1}\bar{1}]$ direction, for $N = 8$, we estimate a value of about $0.041I_c$, possibly dependent on the initial phase configuration. In both cases, our calculated critical currents are in reasonable agreement with those obtained by Bobbert⁷, using a piece-wise linear function to approximate the sinusoidal coupling function.

The array critical current at field $f = 1/(2N^2)$ can be interpreted as the depinning current of a single vortex. It is of interest to compare our calculated value with the energy barrier for depinning. This energy barrier was calculated by Lobb *et al.*¹⁶, who used static methods to obtain a value of about $0.043\hbar I_c/(2e)$. This represents the energy which must be overcome in order to move a vortex from the center of one triangular plaquette to the center of an adjacent plaquette.

To make this comparison, and also to account for the apparent isotropy of the vortex depinning current, we have used a simple model for the vortex potential $U(\mathbf{r})[\mathbf{r} \equiv (x, y)]$. Since $U(x, y)$ must have the array periodicity, we express it as a Fourier series involving only Fourier components from the reciprocal lattice. The sim-

plest approximation consistent with the point symmetry of the lattice is to include only the smallest-magnitude Fourier components, i. e.

$$U(\mathbf{r}) = U_0 + U_1 \sum_{\mathbf{K}} \cos(\mathbf{K} \cdot \mathbf{r}) \quad (6)$$

where we take $U_1 > 0$ and \mathbf{K} is one of the six smallest reciprocal lattice vectors. ($\mathbf{r} = 0$ is interpreted as a grain center, and hence a maximum in the potential.) The potential barrier for vortex depinning in this model is readily shown to be just U_1 .

To estimate the critical current in this picture, we add to the vortex potential energy a term $|\Phi_0 \mathbf{J} \times \mathbf{r}|/c$, where \mathbf{J} is the external current density. This term corresponds to the Magnus force $\mathbf{J} \times \hat{\mathbf{z}} \Phi_0/c$ on a single vortex. When this term is included, we find numerically that the barrier for vortex motion between adjacent triangular plaquettes disappears at $a\hbar J/(2e) \approx 0.984U_1$ for current injected in the $[10\bar{1}]$ direction. Taking $U_1 = 0.043\hbar I_c/(2e)$ from the results of Lobb *et al.*¹⁶, and using $J = I/a$ for $[10\bar{1}]$ current injection, we see that our calculated vortex depinning current of $0.042I_c$ is in excellent agreement with the static results. This calculation also suggests that expression (6) is a reasonable approximation for the vortex potential.

IV. SINGLE VORTEX MOTION: NUMERICAL RESULTS

As shown in Fig. 3 and Fig. 4, the $I - \langle V \rangle$ characteristics display a long low voltage tail at currents above the vortex depinning current. This current regime is approximately Ohmic. Since the $I - \langle V \rangle$ characteristics in this region can be understood in terms of single vortex motion in the array, this region is often called the flux flow regime⁷⁻⁹.

At $\beta = 0$, the flux flow regime extends to about $1.9I_c$ and $1.5I_c$ for current biased in the $[10\bar{1}]$ and $[2\bar{1}\bar{1}]$ directions. Both of these values are close to the critical current of the array at $f = 0$. Above these currents, the whole array is depinned and the vortex picture is not applicable. At sufficiently large values of β , with the current injected at $[10\bar{1}]$ direction, the flux flow regime terminates at lower currents, where there is a ‘‘row switching’’ event^{15,17} rather than the depinning of the entire array – that is, one or more rows of junctions parallel to the direction of current injection switch from the supercurrent state to the resistively dissipative state. This occurs, for

example, near $I = 1.5I_c$ at $\beta = 10$ in 8×8 array. Above this row-switching threshold, the picture of ohmic resistance by flux flow of vortices is no longer valid. At yet higher β values, the flux flow regime terminates at smaller currents, and there may be more than one row switching event before the entire array is depinned. At $\beta = 100$ in 8×8 array, for example, we find two row switching events in our calculations. As in Ref. 9, we also find the staircase-like structure in the $I - \langle V \rangle$ curve in the flux flow region, which may arise from the interaction of the vortex with its image neighboring vortices generated by the periodic boundary conditions.

Figs. 5(a) and 5(b) show the time-dependent space-averaged voltage drop $V(t)$ across the array – that is, the difference between the average voltage on the line of grains where the current is injected, and the line from which it is extracted – at two current values in the flux-flow regime. In both cases, $\beta = 0$ and the current is injected in the $[10\bar{1}]$ direction. $V(t)$ is characterized by periodic sharp peaks which resemble the time-dependent voltage of a single junction, the frequency of which increases with increasing bias current.

If the single vortex picture is correct, the spike frequency ν_v is related to $\langle V \rangle$. The period of oscillation should correspond to the motion of a vortex by one unit cell. Furthermore, a complete vortex circuit around the lattice should produce a phase change of 2π across the array. Then using the Josephson relation, we obtain

$$\langle V \rangle = \frac{\hbar}{2e} \left\langle \frac{d}{dt} \phi \right\rangle = \frac{\hbar}{2e} \frac{2\pi}{T}, \quad (7)$$

where T is the period for one complete vortex circuit. For an $N \times N$ array, $T = N/\nu_v$. Our numerical results are in excellent agreement with this relation, thus confirming the vortex motion picture in the flux flow regime.

By examining the time-dependent voltage of each single junction, one can also deduce the actual vortex path in the array. This path is displayed in Fig. 5(c) for an 8×8 array with bias current in the $[10\bar{1}]$ direction. We find that this path is independent of current magnitude in the $[10\bar{1}]$ direction. As shown in the figure, it is a straight trajectory through the middle of the array.

The behavior of vortices is more complex when current is applied in the $[2\bar{1}\bar{1}]$ direction. In this case, the flux flow regime in an 8×8 overdamped array consists of three distinct subregions with different slopes as shown in Fig. 4. A typical voltage trace $V(t)$ from each subregion is shown in Figs. 6(a), 6(b), and 6(c). The relationship between spike frequency and time-averaged voltage still holds, im-

plying that the picture of vortex motion is still correct in this direction. However, the vortex path is different in each of the three subregions. These paths, as deduced from the time-dependent voltages of each junction, are shown in Figs. 6(d), 6(e), and 6(f).

At sufficiently low bias current in $[10\bar{1}]$ direction, $V(t)$ shows a double-peaked structure. We believe that this structure originates in the special geometry of the triangular lattice, in which each primitive cell has two triangular plaquettes which are inequivalent. When a bias current is applied in the $[10\bar{1}]$ direction, the vortex will pass alternately through each of these plaquettes, somehow producing a double-peaked structure in $V(t)$. As the bias current increases, the double-peaked structure in $V(t)$ seems to disappear. However, the time-dependent voltage of each individual junction still exhibits a double-peaked structure. The disappearance of the double-peak structure in $V(t)$ is therefore due to space-averaging. We conclude that our simple vortex potential is qualitatively correct even at higher bias current. Of course, above the array depinning current ($I = 2I_c$ for this direction), the vortex picture breaks down and $V(t)$ shows no simple behavior, just as was found previously for square arrays^{9,14}.

V. FLUX FLOW RESISTIVITY AND VORTEX FRICTION COEFFICIENT

As noted above, in the flux flow regime, the Josephson network behaves approximately ohmically. In this ohmic regime, we can define a *vortex friction coefficient* η by equating the driving force $J\Phi_0/c$ to the frictional drag force ηv , where v is the vortex velocity. This gives (assuming current injected in the $[10\bar{1}]$ direction)

$$\eta v \equiv \frac{2\pi \hbar}{a} \frac{I}{2e}, \quad (8)$$

where $I = aJ$ is the current injected into one node.

This vortex friction coefficient can be estimated in a simple way by equating the frictional losses to the power dissipated in the shunt resistances when the vortex moves with constant velocity. The result of this procedure for a square array is³

$$(\eta_0)_{sq} = \left(\frac{\hbar}{2e} \right)^2 \left(\frac{2\pi}{a} \right)^2 \frac{1}{2R}, \quad (9)$$

and for a triangular array (cf. Appendix A),

$$(\eta_0)_{tri} = 2 \left(\frac{\hbar}{2e} \right)^2 \left(\frac{2\pi}{a} \right)^2 \frac{1}{2R}. \quad (10)$$

η can also be obtained directly from the calculated I - $\langle V \rangle$ characteristics (cf. Appendix B). Our numerical results for different values of β in 8×8 arrays are shown in Table 2. This Table shows that η varies approximately as $\beta^{1/2}$ at large β values, and differs considerably from the result (10). Indeed, at sufficiently large values of β , the friction coefficient actually appears to be independent of the shunt resistance R . A similar result was also found previously in square arrays.⁷⁻⁹

A more accurate theoretical calculation of the frictional damping requires taking account of the loss of vortex energy to “spin-wave-like” excitations in the array. A continuum theory of this kind has been proposed by Geigenmüller *et al*.⁹ In Appendix C, we give a detailed, quasi-analytical theory for the friction coefficient, based on the loss of energy from a vortex moving with velocity \mathbf{v} to spin wave modes. The model is more general than that of Ref. 9, in that it takes explicit account of the lattice structure of the array, so that a short-wavelength cutoff appears naturally, and allows for an arbitrary external current source to excite the spin wave modes (for example, one arising from a high density of vortices). The final result for η in a square array is

$$\left(\frac{\eta}{(\eta_0)_{sq}} \right) = \frac{1}{2\pi^2} I', \quad (11)$$

and in a triangular array

$$\left(\frac{\eta}{(\eta_0)_{tri}} \right) = \frac{\sqrt{3}}{8\pi^2} I', \quad (12)$$

where the dimensionless integral I' is given in Appendix C.

It is sometimes useful to transform η into an analogous expression for array resistivity. Using the force balance equation (8), and noting that the electric field has magnitude $E = 2\pi(\hbar/(2e))n_v v$, where $n_v = 4f/(\sqrt{3}a^2)$ is the number of vortices per unit area, we obtain Ohm’s Law in the form

$$\mathbf{E} = \rho \mathbf{J},$$

where the array resistivity is (after considerable simplification)

$$\rho = \frac{32\pi^2 f R}{3I'}. \quad (13)$$

Table 3 shows the friction coefficient as calculated from the model of Appendix C. As can be seen, the resulting coefficient is strongly dependent upon β , in agreement

with our numerical “experiment.” If, for example, we choose the scaled vortex velocity $\tilde{v} = 1.0$ (as defined in Eq. (32)), our analytic expression for η is well approximated in square array by the simple expression

$$\eta \approx 0.89\beta^{1/2}(\eta_0)_{sq}, \quad (14)$$

and in a triangular array by

$$\eta \approx 0.34\beta^{1/2}(\eta_0)_{tri}. \quad (15)$$

The $\beta^{1/2}$ trend is consistent with the results of numerical calculations in Ref. 9 for square arrays and in the present work for triangular arrays, although the numerical coefficient may differ by as much as a factor of two. The trend is also consistent with the experimental results of Ref. 8. Note that $\tilde{v} = 1$ is a reasonable velocity to consider in this comparison, because larger velocities tend to trigger row-switching events in underdamped arrays.^{7-10,15,23}

Table 3 also lists the variation of η with \tilde{v} at several values of β . Evidently, η is nearly independent of \tilde{v} at large \tilde{v} but goes to zero below a threshold value of order $\tilde{v} = 0.2$, where the damped pole in the integral (31) moves outside the first Brillouin zone of the triangular lattice. Once again, this agrees with the results found in the continuum theory of Ref. 9 for a square lattice. The results also agree quite well with our numerical results, as shown by a comparison of Tables 2 and 3(b).

VI. ABSENCE OF BALLISTIC VORTEX MOTION

A rather surprising result of our simulations is the absence of ballistic vortex motion. Such motion might have been expected, at least in the highly-underdamped regime; and there have been some experimental reports of such behavior^{4,6}. In order to check for ballistic motion, we apply a large bias current to the array in the flux flow regime, so that the vortex acquires a high initial velocity, then we turn off the bias current. Since the effective mass of the vortex is presumably large in the high- β regime, the vortex might be expected to move several lattice spacings because of its large initial kinetic energy, even after the driving current is removed. But from the calculated time-dependent voltage of the individual junctions, we find that the vortex travels at most through one primitive cell after the bias current is shut off, whatever its initial velocity, for all values of β considered ($0 \leq \beta \leq 1000$). This is consistent with previous calculations⁷.

It is of some interest to compare our results with those of Ref. 10. This paper considers the triangular array in a continuum approximation and concludes that a narrow vortex velocity window exists where ballistic motion is possible. It is suggested that this window extends from the vortex depinning current to roughly twice that current. We can envision two possible reasons why we do not see this ballistic regime in our own calculations. The first is that the depinning current is rather dependent on lattice size, typically being larger for the smaller lattices. For our size regime, this may narrow the window nearly to zero. In addition, the vortex velocity is not constant just above the depinning current, but instead is quite time-dependent, because of the periodic pinning potential. This time dependence is not considered in the model of ref. 10, which assumes a constant vortex velocity in estimating the width of the ballistic “window.” Thus, the effects of this time-dependence could possibly also suppress this window.

In view of these results, the explanation for the ballistic motion which is observed in experiments seems unclear. No numerical calculation has yet found such motion from classical equations. Conceivably, the ballistic regime arises when quantum effects reduce the vortex friction coefficient below classical predictions, but this remains to be proven.

VII. DISCUSSION AND CONCLUSIONS

We have simulated the dynamical response of triangular Josephson junction arrays, using a classical model of resistively- and capacitively-shunted Josephson junctions described by coupled second-order differential equations. In the flux flow regime, the dynamical response of the network, including the time-dependent voltage, is well described in terms of vortex degrees of freedom. The vortices, however, experience higher viscous damping than predicted on the basis of a simplified model, and in apparent contrast to experiment do not exhibit ballistic motion at any bias current we have investigated. The damping is reasonably well described, however, by a model which describes loss of vortex energy to plasma (or “phase wave”) oscillations in the Josephson network.

It is of interest to make a crude estimate of the pa-

rameters where quantum corrections might need to be included in these calculations. In a naive picture, such corrections would start to matter when the characteristic charging energy $(2e)^2/C$ becomes comparable to the Josephson energy $\hbar I_c/(2e)$. This condition gives

$$CI_c \approx \frac{(2e)^3}{\hbar}. \quad (16)$$

This can be translated into a condition on the lattice resistivity, using Eqs. (12), (13), and (15), with the result

$$\rho \propto f \left(\frac{\hbar}{(2e)^2} \right), \quad (17)$$

where the constant of proportionality is approximately 1.1. This result suggests that quantum corrections might become important when the resistance per square of this two-dimensional network is comparable to the “quantum of resistance” $h/(2e)^2$ per unit frustration. Of course, this naive estimate does not take account of such obvious corrections as vortex-vortex interactions. It is amusing to note that several groups have reported evidence (both experimental and theoretical²⁴) for a superconductor-to-insulator transition in quasi-two-dimensional superconductors in a magnetic field at a resistance per square of order $h/(2e)^2$; this transition is generally attributed to disorder effects, and thus may be unrelated to the simple criterion for arrays mentioned above. Thus a detailed calculation of quantum effects on vortex motion remains an important problem for future study.

VIII. ACKNOWLEDGMENTS

We gratefully acknowledge support by the National Science Foundation through Grant DMR 90-20994. Our calculations were carried out, in part, on the CRAY Y-MP 8/864 of the Ohio Supercomputer Center, with the help of a grant of time which we gratefully acknowledge.

APPENDIX A: SIMPLE ESTIMATE OF VORTEX FRICTION COEFFICIENT

In this Appendix, we present a simple estimation of the friction coefficient for a single vortex moving in a triangular array. If we assume that such a vortex moves from the center of one plaquette to the center of a nearest-neighbor plaquette, it must cross one junction. Since the change in phase difference is $2\pi/3$ when the vortex crosses the junction, the average voltage across the junction is

$$\langle V \rangle = \frac{\hbar}{2e} \cdot \frac{2\pi/3}{\Delta t} = \frac{\hbar}{2e} \cdot \frac{2\pi/3}{\frac{\sqrt{3}}{3}a/v} = \frac{2}{\sqrt{3}} \cdot \frac{\hbar}{2e} \cdot \frac{\pi}{a} \cdot v,$$

where Δt is the time required for the vortex to move from one plaquette center to the next, a is the lattice constant, and v is the time-averaged vortex velocity.

We next compute the effective frictional coefficient by equating the resistively dissipated energy to that expected for a particle moving in a viscous medium. Now the effective resistance between two nearest neighbor grains is defined as the voltage drop which is produced when a unit current is injected into one such grain and extracted from the other. Since there are six nearest neighbors in a triangular lattice, the effective resistance in an infinite triangular array is $R/3$, where R is the single-junction resistance.²⁵ Equating the resistively dissipated power to the frictional losses, we obtain

$$\frac{1}{2}(\eta_0)_{tri}v^2 = \frac{\langle V \rangle^2}{2(R/3)} = \frac{3}{2R} \cdot \frac{4}{3} \cdot \left(\frac{\hbar}{2e}\right)^2 \cdot \left(\frac{\pi}{a}\right)^2 \cdot v^2.$$

This implies that the vortex frictional coefficient in an infinite triangular array is

$$(\eta_0)_{tri} = 2 \cdot \left(\frac{\hbar}{2e}\right)^2 \cdot \left(\frac{2\pi}{a}\right)^2 \cdot \frac{1}{2R}. \quad (18)$$

A similar calculation for a square array gives^{3,5}:

$$(\eta_0)_{sq} = \left(\frac{\hbar}{2e}\right)^2 \cdot \left(\frac{2\pi}{a}\right)^2 \cdot \frac{1}{2R}. \quad (19)$$

APPENDIX B: EXTRACTION OF η FROM $I - \langle V \rangle$ CHARACTERISTICS

In the flux flow region, the time- and space-averaged voltage $\langle V \rangle$ across an $M \times N$ array is approximately proportional to the bias current I . We define a dimensionless proportionality coefficient γ by

$$\langle V \rangle = \gamma N R I,$$

where N is the number of junctions along the direction of the bias current. If we assume periodic transverse boundary conditions and $[10\bar{1}]$ current injection, a complete circuit of a vortex around the array produces a phase change of 2π across the array in the direction parallel to the current injection. The Josephson relation then implies that

$$\langle V \rangle = \frac{\hbar}{2e} \left\langle \frac{d\phi}{dt} \right\rangle = \frac{\hbar}{2e} \frac{2\pi}{M a} v,$$

where a is the lattice constant and v is the transverse vortex velocity. Since the friction coefficient η_{tri} is related to v by Eq. (8), we obtain, on combining the above relations,

$$\begin{aligned} \eta_{tri} &= \frac{2}{\gamma M N} \cdot \left(\frac{\hbar}{2e}\right)^2 \cdot \left(\frac{2\pi}{a}\right)^2 \cdot \frac{1}{2R} \\ &= \frac{1}{\gamma M N} (\eta_0)_{tri}. \end{aligned} \quad (20)$$

APPENDIX C: ANALYTICAL MODEL FOR VORTEX FRICTION COEFFICIENT

We consider a d-dimensional periodic network of RCSJ's, assuming zero shunt capacitance to ground, and also assuming that the shunt resistance, junction critical current, and shunt capacitance all vanish except between nearest neighbors, for which they take the values R , I_c , and C respectively.

With these assumptions, the equations of motion for the phases may be written in the form

$$\frac{\hbar}{2e} C \sum_j \ddot{\phi}_{ij} + \frac{\hbar}{2eR} \sum_j \dot{\phi}_{ij} + I_c \sum_j \sin(\phi_{ij}) = I_{i,ext}, \quad (21)$$

where the sums run over the nearest neighbors to the grain i and $\phi_{ij} = \phi_i - \phi_j$.

We will calculate the losses produced by an externally applied current due to excitation of "spin waves", i. e. small-amplitude phase fluctuations. Thus, we expand the sine-function as $\sin(\phi_i - \phi_j) \approx \phi_i - \phi_j$, and, within that assumption, calculate the losses coming from an arbitrary $I_{i,ext}(t)$. With the introduction of the Fourier transforms $\phi(\mathbf{k}, \omega)$ and $I_{ext}(\mathbf{k}, \omega)$, we can transform (21) into the form

$$\phi(\mathbf{k}, \omega) = \frac{I_{ext}(\mathbf{k}, \omega)/t(\mathbf{k})}{I_c - \frac{i\hbar\omega}{2eR} - \frac{\hbar\omega^2 C}{2e}}. \quad (22)$$

Here

$$t(\mathbf{k}) = \sum_{nn} (1 - \exp(i\mathbf{k} \cdot \mathbf{R})),$$

the sum runs over the set of nearest neighbor lattice vectors \mathbf{R} , and the allowed \mathbf{k} values run over the first Brillouin zone of the grain lattice.

The energy dissipation in the ij^{th} bond in the time interval $[-T, T]$ is:

$$\Delta E_{ij} = \int_{-T}^{+T} I_{ij}(t) V_{ij}(t) dt,$$

or, in Fourier transform,

$$\Delta E_{ij} = \int_{-\infty}^{\infty} d\omega \int_{-\infty}^{\infty} d\omega' I_{ij}(\omega) V_{ij}^*(\omega') A(\omega, \omega'), \quad (23)$$

where

$$A(\omega, \omega') = \frac{1}{\pi} \frac{\sin[(\omega - \omega')T]}{\omega - \omega'}.$$

The total energy loss $\Delta E_{tot} \equiv \sum_{\langle ij \rangle} \Delta E_{ij}$. Using the Josephson relation between phase and voltage, and the equations of motion (21) in the small phase difference approximation, and making the relevant Fourier transforms, we can finally express the total energy loss as

$$\begin{aligned} \Delta E_{tot} &= \frac{\hbar}{2eN} \sum_{\mathbf{k}} \frac{1}{t(\mathbf{k})} \int_{-\infty}^{\infty} d\omega \int_{-\infty}^{\infty} d\omega' \times \\ &\times \Re \frac{i\omega' I_{ext}(\mathbf{k}, \omega) I_{ext}^*(\mathbf{k}, \omega')}{I_c + \frac{i\hbar\omega'}{2eR} - \frac{\hbar\omega'^2 C}{2e}} A(\omega, \omega'), \end{aligned} \quad (24)$$

where N is the number of grains in the lattice, and the sum runs over the first Brillouin zone.

This result is valid for an arbitrary external current source. We now specialize to a vortex moving with velocity \vec{v} . According to Geigenmüller *et al*, such a vortex traveling in the y direction has associated with it a charge density

$$Q^V(\mathbf{x}, t) = C \frac{\hbar}{2e} v \frac{\partial}{\partial x} 2\pi \delta(x) \delta(y - vt).$$

The corresponding space and time Fourier transform is:

$$Q^V(\mathbf{k}, \omega) = (2\pi)^{3/2} C \frac{\hbar}{2e} v (-ik_x) \delta(\omega - vk_y). \quad (25)$$

Of course, this charge density was derived for a vortex moving in a *continuum* superconductor, and cannot be exactly correct for a superconducting array. However,

by imposing the additional requirement that $Q^V(\mathbf{k}, \omega)$ vanish for \mathbf{k} outside the first Brillouin zone, we produce an approximate charge density which is properly discrete.

The external current corresponding to this charge distribution is:

$$I_{ext}(\mathbf{k}, \omega) = -i\omega Q^V(\mathbf{k}, \omega).$$

We substitute this into Eq. (24) and convert the sum over \mathbf{k} into an integral, with the help of a factor $S/(4\pi^2)$, where S is the area of the array. The integrand vanishes unless $\omega = \omega'$. Next, we explicitly evaluate the real part, using the fact that $A(\omega, \omega) = \frac{T}{\pi}$, and dividing by $2T$. The two integrals over frequency can be done immediately, since they involve delta-functions, and the final result for the time rate of energy loss from the vortex into the spin wave modes reduces to

$$\frac{dE}{dt} = \eta v^2, \quad (26)$$

where η is an effective vortex friction coefficient. The form (26) properly corresponds to a frictional force of the form $-\eta v$, since the rate of energy loss is the dot product of the force with the velocity.

The expression for η can be written most compactly by using the dimensionless variables $k'_i = ak_i$, $i = x$ or y , where a is the bond length. We also introduce a dimensionless vortex velocity

$$\tilde{v} = v/(a\omega_0), \quad (27)$$

where $\omega_0 = \sqrt{2eI_c/\hbar C}$ is the Josephson plasma frequency. After some algebra, we obtain Eqs. (11) and (12), respectively, for η in a square array and a triangular array. In both cases the dimensionless integral I' takes the form

$$I'(\tilde{v}, \beta) = \int_{B.Z.} dk'_x dk'_y \left(\frac{(k'_x)^2 (k'_y)^4}{[1/\tilde{v}^2 - (k'_y)^2]^2 + \frac{(k'_y)^2}{\tilde{v}^2 \beta}} \right) \left(\frac{1}{t(k'_x, k'_y)} \right), \quad (28)$$

and $(\eta_0)_{sq}$ and $(\eta_0)_{tri}$ are given by Eq. (9) and Eq. (10). The integral for both lattices runs over the scaled first Brillouin zone of the array (defined by taking the bond length $a = 1$).

REFERENCES AND FOOTNOTES

1. For many references up to 1988, see, e. g., the articles in *Physica (Amsterdam)* **152B**, pp. 1-302 (1988). For some recent reviews, see, e. g., the articles in *Proceedings of the 2nd CTP Workshop on Statistical Physics: KT Transition and Superconducting Arrays*, edited by D. Kim, J. S. Chung, and M. Y. Choi (Min Eum Sa, Seoul, Korea, 1993).
2. U. Eckern and A. Schmid, *Phys. Rev.* **B39**, 6441 (1989).
3. M. S. Rzchowski, S. P. Benz, M. Tinkham and C. J. Lobb, *Phys. Rev.* **B42**, 2041 (1990).
4. H. S. J. van der Zant, F. C. Fritschy, T. P. Orlando and J. E. Mooij, *Physica* **B165-66**, 969 (1990).
5. T. P. Orlando, J. E. Mooij and H. S. J. van der Zant, *Phys. Rev.* **B43**, 10218 (1991).
6. H. S. J. van der Zant, F. C. Fritschy, T. P. Orlando and J. E. Mooij, *Europhys. Lett.* **18**, 343 (1992).
7. P. A. Bobbert, *Phys. Rev.* **B45**, 7540 (1992).
8. H. S. J. van der Zant, F. C. Fritschy, T. P. Orlando and J. E. Mooij, *Phys. Rev.* **B47**, 295 (1993).
9. U. Geigenmüller, C. J. Lobb, C. B. Whan, *Phys. Rev.* **B47**, 348 (1993).
10. U. Eckern and E. B. Sonin, *Phys. Rev.* **B47**, 505 (1993).
11. B. J. Van Wees, *Phys. Rev. Lett.* **65**, 255 (1990).
12. T. P. Orlando and K. A. Delin, *Phys. Rev.* **B43**, 8717 (1991).
13. R. Théron, J.-B. Simond, Ch. Leemann, H. Beck, P. Martinoli, and P. Minnhagen, *Phys. Rev. Lett.* **71**, 1246 (1993).
14. Wenbin Yu, K. H. Lee and D. Stroud, *Phys. Rev.* **B 47**, 5906 (1993).
15. Wenbin Yu and D. Stroud, *Phys. Rev.* **B 46**, 14005 (1992).
16. C. J. Lobb, D. W. Abraham and M. Tinkham, *Phys. Rev.* **B27**, 150 (1983).
17. H. S. J. van der Zant, C. J. Muller, L. J. Geerligs, C. J. P. M. Harmans and J. E. Mooij, *Phys. Rev.* **B38**, 5154 (1988).
18. T. S. Tighe, A. T. Johnson and M. Tinkham, *Phys. Rev.* **B44**, 10286 (1991).
19. D. E. McCumber, *J. Appl. Phys.* **39**, 3113 (1968); W. C. Stewart, *Appl. Phys. Lett.* **22**, 277 (1968).
20. L. L. Sohn, M. S. Rzchowski, J. U. Free, M. Tinkham, and C. J. Lobb, *Phys. Rev.* **B45**, 3003 (1992).
21. There have been, by now, a very large number of dynamical calculations based on similar sets of coupled equations. Some representative calculations are: K. K. Mon and S. Teitel, *Phys. Rev. Lett.* **62**, 673 (1989); A. Falo *et al*, *Phys. Rev.* **B41**, 10983 (1990); T. C. Halsey, *Phys. Rev.* **B41**, 11634 (1990); W. Xia and P. L. Leath, *Phys. Rev. Lett.* **63**, 1428 (1989); H. Eikmans and J. E. van Himbergen, *Phys. Rev.* **B41**, 8927 (1990); L. L. Sohn *et al*, *Phys. Rev.* **B44**, 925 (1991); D. Dominguez *et al*, *Phys. Rev. Lett.* **67**, 2367 (1991); M. Octavio *et al*, *Phys. Rev.* **B44**, 4601 (1991); K. Y. Tsang *et al*, *Phys. Rev. Lett.* **66**, 1094 (1991); R. Bhagavatula *et al*, *Phys. Rev.* **B45**, 4774 (1992); S. R. Shenoy, *J. Phys.* **C18**, 5163 (1985).
22. Quantum effects have been discussed by many authors, starting with P. W. Anderson, in *Lectures on the Many Body Problem*, edited by E. R. Caianello (Academic Press, New York 1964), Vol II; B. Abeles, *Phys. Rev.* **B15**, 2828 (1977); and E. Simanek, *Solid State Commun.* **31**, 419 (1979). For further references, see, e. g., G. Schön in Ref. 1, and references therein.
23. This criterion for the excitation of spin waves was pointed out long ago, in the context of a continuum model, by K. Nakajima and Y. Sawada, *J. Appl. Phys.* **52**, 5732 (1981).
24. M. P. A. Fisher, *Phys. Rev. Lett.* **65**, 923 (1990); A. F. Hebard and M. A. Paalanen, *Phys. Rev.* **65**, 927 (1990); E. S. Sorenson *et al*, *Phys. Rev. Lett.* **69**, 828 (1992).
25. S. Kirkpatrick, *Rev. Mod. Phys.* **45**, 574 (1973).

FIGURE CAPTIONS

the periodic boundary conditions are represented by repeating the $N \times N$ lattice.

1. Schematic diagram of an 8×8 triangular Josephson junction array. Each intersection represents a superconducting grain, which is connected to its six nearest neighbors by Josephson coupling. (a) and (b) correspond respectively to $[10\bar{1}]$ and $[2\bar{1}\bar{1}]$ current injection direction. Free boundary conditions are used in the direction of current injection, while periodic boundary conditions are used in the transverse direction.
2. Schematic illustration of a triangular plaquette of Josephson junctions at zero magnetic field, subjected to an injected current I as shown. The critical current for this arrangement is $1.7602I_c$.
3. $I - \langle V \rangle$ characteristics for 8×8 triangular arrays at $f = 1/128$ at two different β values with current injected in the $[10\bar{1}]$ direction: (a) $\beta = 0$; (b) $\beta = 10$. The insets are enlargements of the flux flow regime.
4. $I - \langle V \rangle$ characteristics for overdamped 8×8 triangular arrays ($\beta = 0$) at $f = 1/128$ with current injected in the $[2\bar{1}\bar{1}]$ direction. The inset is the enlargement of the flux flow regime.
5. Time dependent voltage traces and vortex motion path in the array for 8×8 overdamped arrays ($\beta = 0$) at $f = 1/128$ with current injected in the $[10\bar{1}]$ direction for two different applied currents. $t_0 = \hbar/(2eRI_c)$ is a natural unit of time. The bias current and time-averaged voltages are (a) $I/I_c = 0.2$, $\langle V \rangle/NRI_c = 2.39 \times 10^{-3}$; (b) $I/I_c = 1.0$, $\langle V \rangle/NRI_c = 1.91 \times 10^{-2}$. (c) Path of vortex motion in this array; the disks represent successive positions of the vortex in the array.
6. Time dependent voltage traces and vortex trajectories in an 8×8 overdamped array ($\beta = 0$) at $f = 1/128$, for three different values of current applied in the $[2\bar{1}\bar{1}]$ direction. $t_0 = \hbar/(2eRI_c)$ is the natural unit of time. The bias currents and time-averaged voltages are (a) $I/I_c = 0.4$, $\langle V \rangle/NRI_c = 4.298 \times 10^{-3}$; (b) $I/I_c = 0.9$, $\langle V \rangle/NRI_c = 1.123 \times 10^{-2}$; and (c) $I/I_c = 1.3$, $\langle V \rangle/NRI_c = 1.978 \times 10^{-2}$. (d), (e), and (f) show the vortex trajectories corresponding to (a), (b), and (c). We draw the trajectories in a “repeated lattice scheme” in which

TABLE CAPTIONS

1. Numerical values of the critical current for an $N \times N$ triangular array at $f = 1/(2N^2)$, for $[10\bar{1}]$ current injection.
2. Numerical values of η as a function of β in an 8×8 triangular array. γ is estimated from the numerical $I - \langle V \rangle$ characteristics of the corresponding arrays. η is calculated from Eq. (20) in Appendix B, and is estimated by drawing a straight line by eye through the $I - \langle V \rangle$ characteristic in the flux-flow regime.
3. Numerical values of η as obtained from the semi-analytical theory of Appendix C at several values of β and \tilde{v} for square and triangular arrays. The values are obtained by use of Eqs. (33) – (35), carrying out the integral numerically.

Table 1

N	8	12	16	24
I_d/I_c	0.090	0.063	0.054	0.048

Table 2

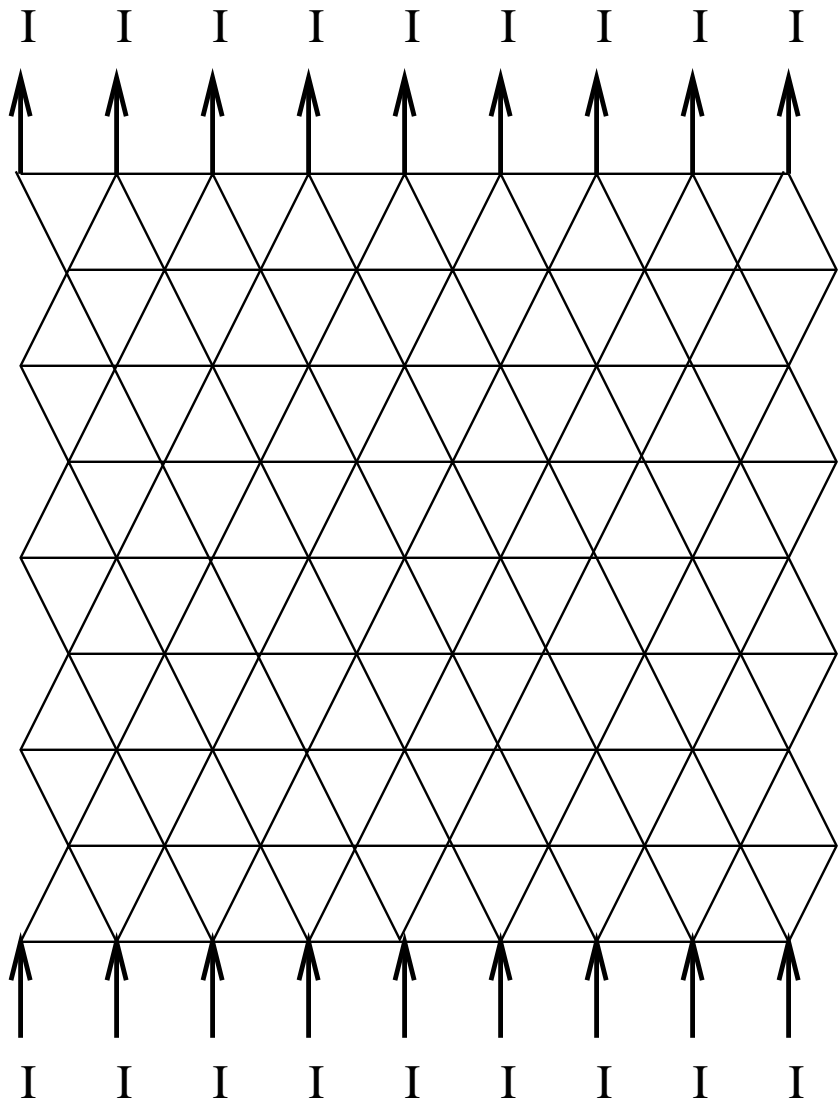
β	γ	η/η_0
0	2.73×10^{-2}	0.572
1	2.13×10^{-2}	0.732
10	8.57×10^{-3}	1.82
50	4.09×10^{-3}	3.82
100	2.78×10^{-3}	5.63
225	2.07×10^{-3}	7.54
400	1.47×10^{-3}	10.7

Table 3 (a)

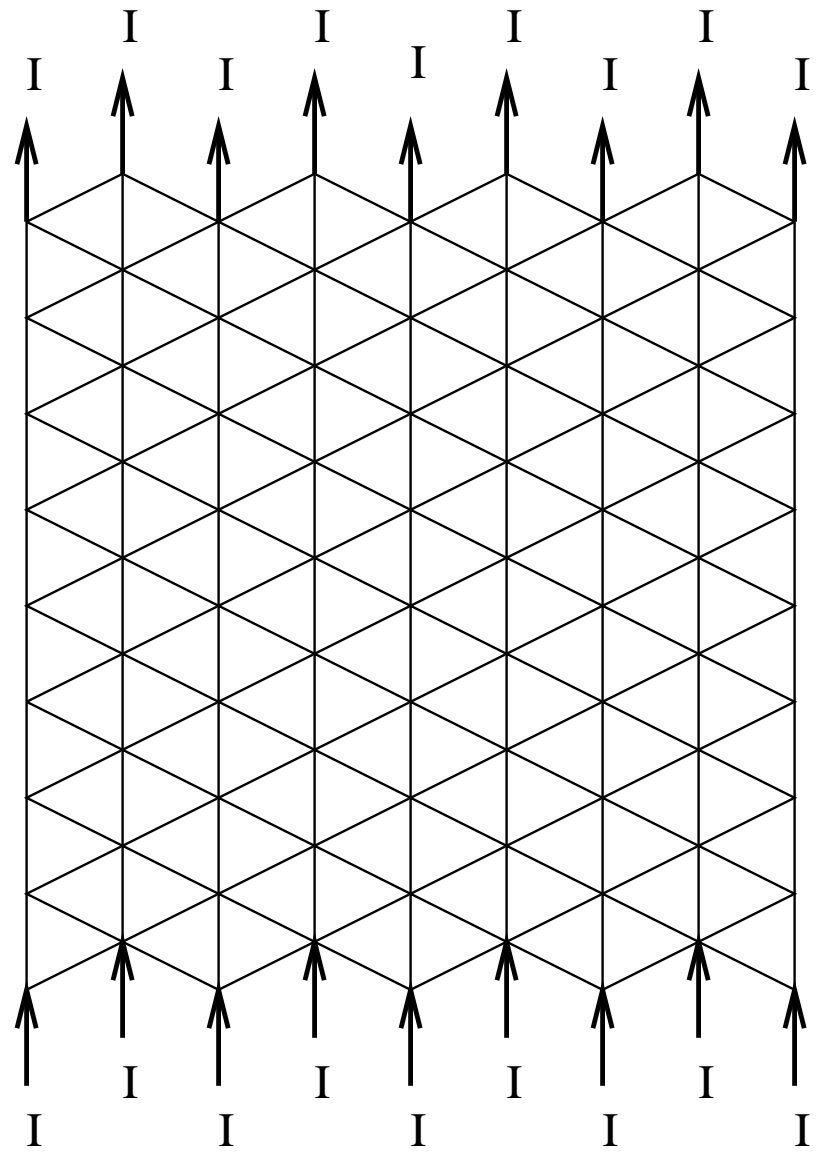
$\eta/(\eta_0)_{sq}$	β						
	1	10	50	100	225	400	
\tilde{v}	0.2	0.040	0.061	0.064	0.064	0.064	0.064
	0.5	0.67	3.16	7.67	11.0	16.7	22.4
	1.0	1.14	3.25	6.75	9.33	13.7	18.2
	2.0	1.38	2.82	5.10	6.83	10.1	14.1

Table 3 (b)

$\eta/(\eta_0)_{tri}$	β						
	1	10	50	100	225	400	
\tilde{v}	0.2	0.014	0.025	0.027	0.027	0.028	0.028
	0.5	0.20	0.94	2.32	3.36	5.13	6.91
	1.0	0.38	1.19	2.55	3.56	5.25	6.84
	2.0	0.48	1.06	1.98	2.66	3.86	5.06

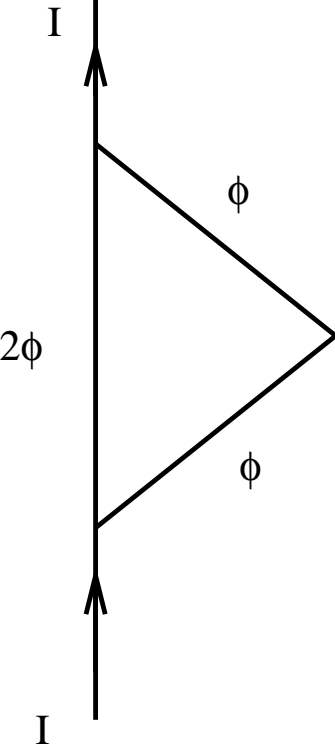


(a)



(b)

Yu at al, Fig. 2



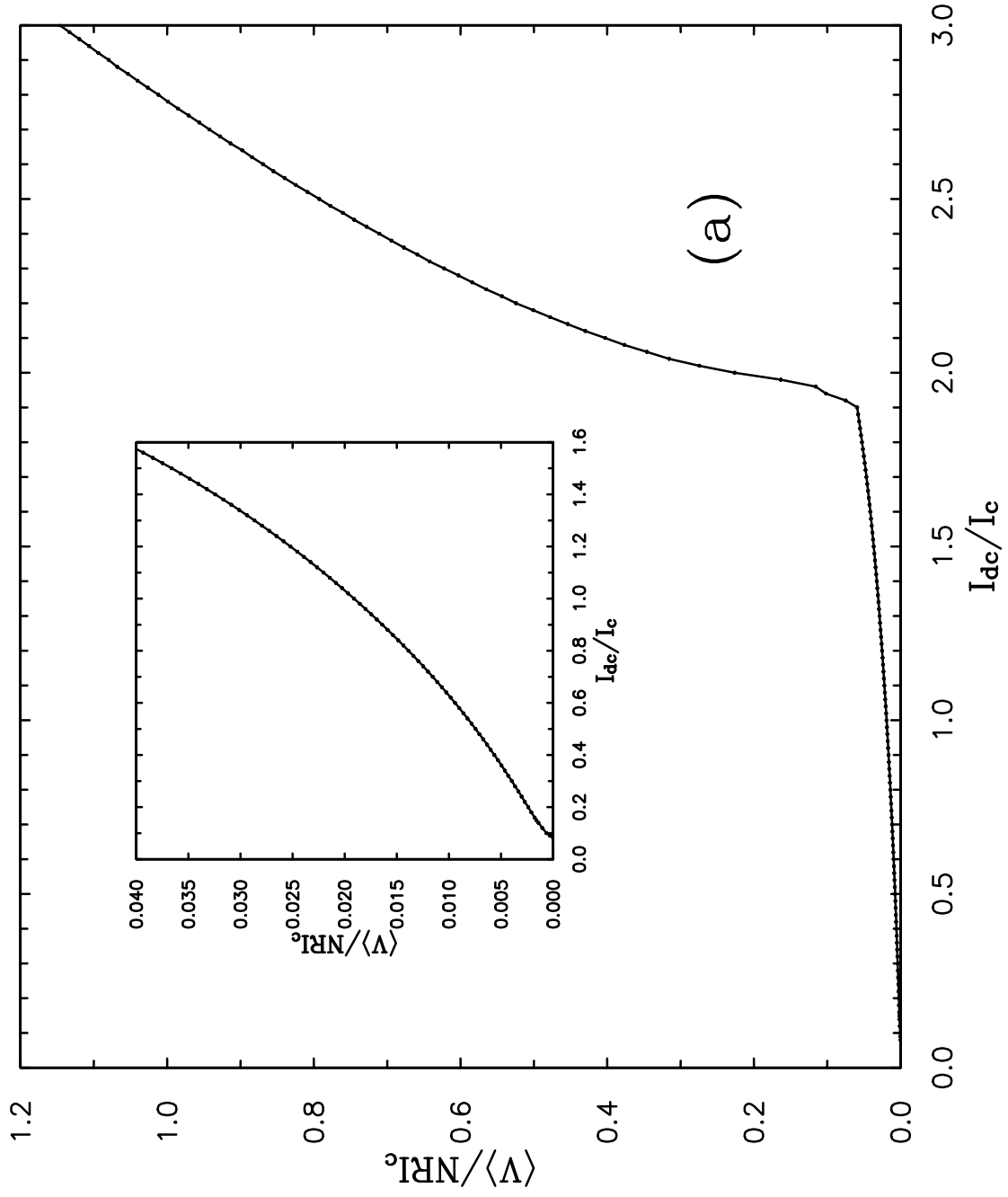


Fig. 3 (a)

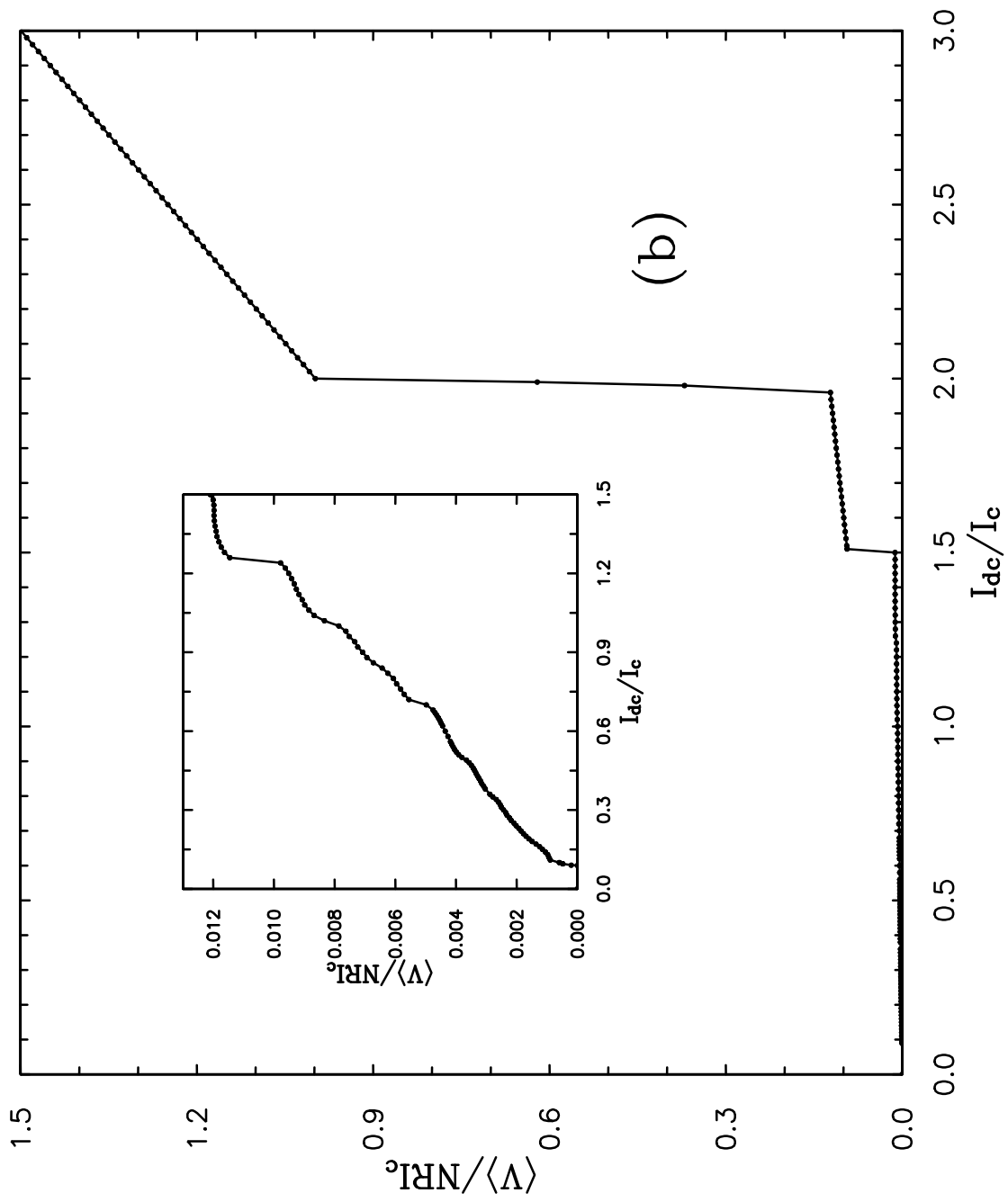


Fig. 3 (b)

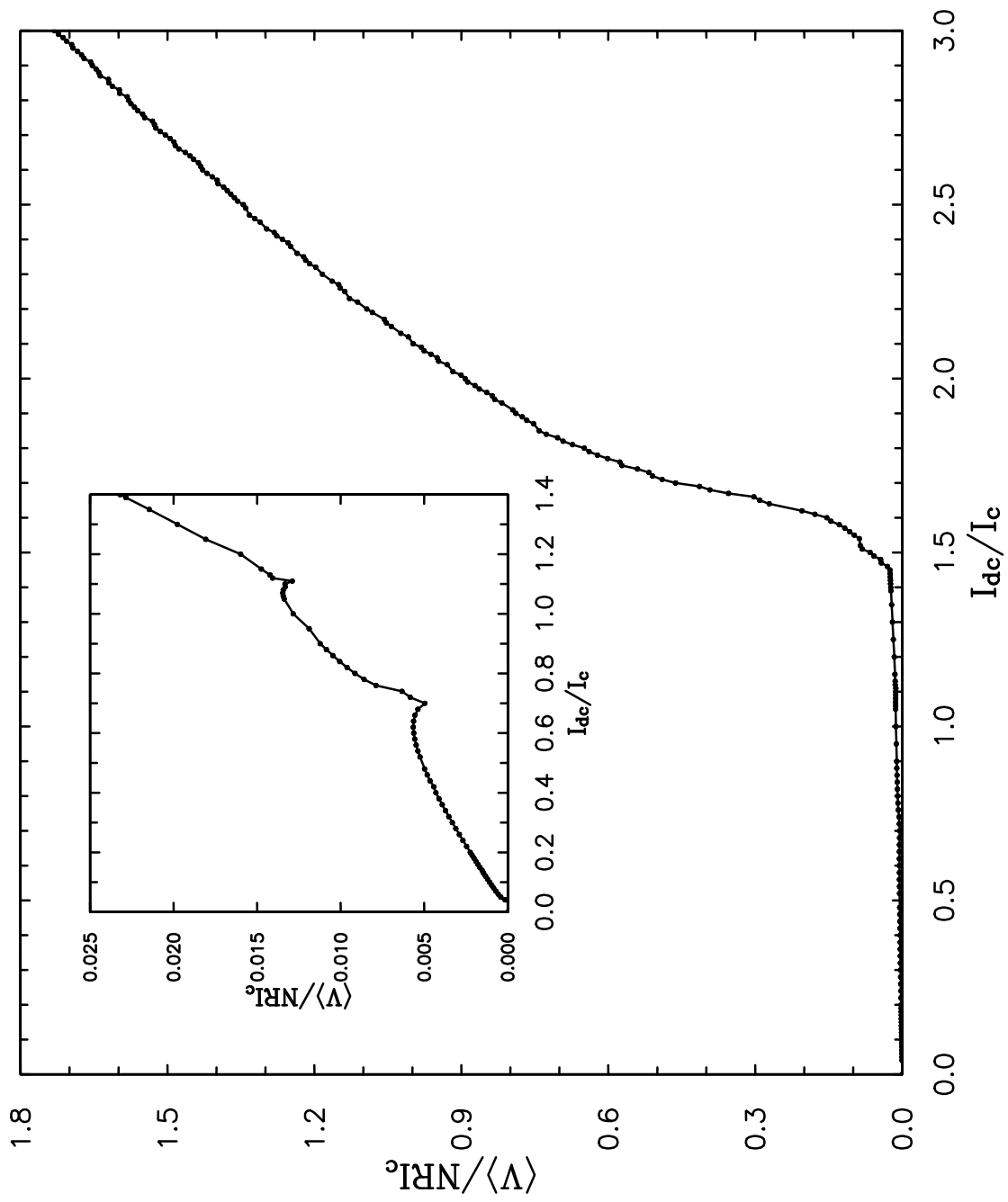


Fig. 4

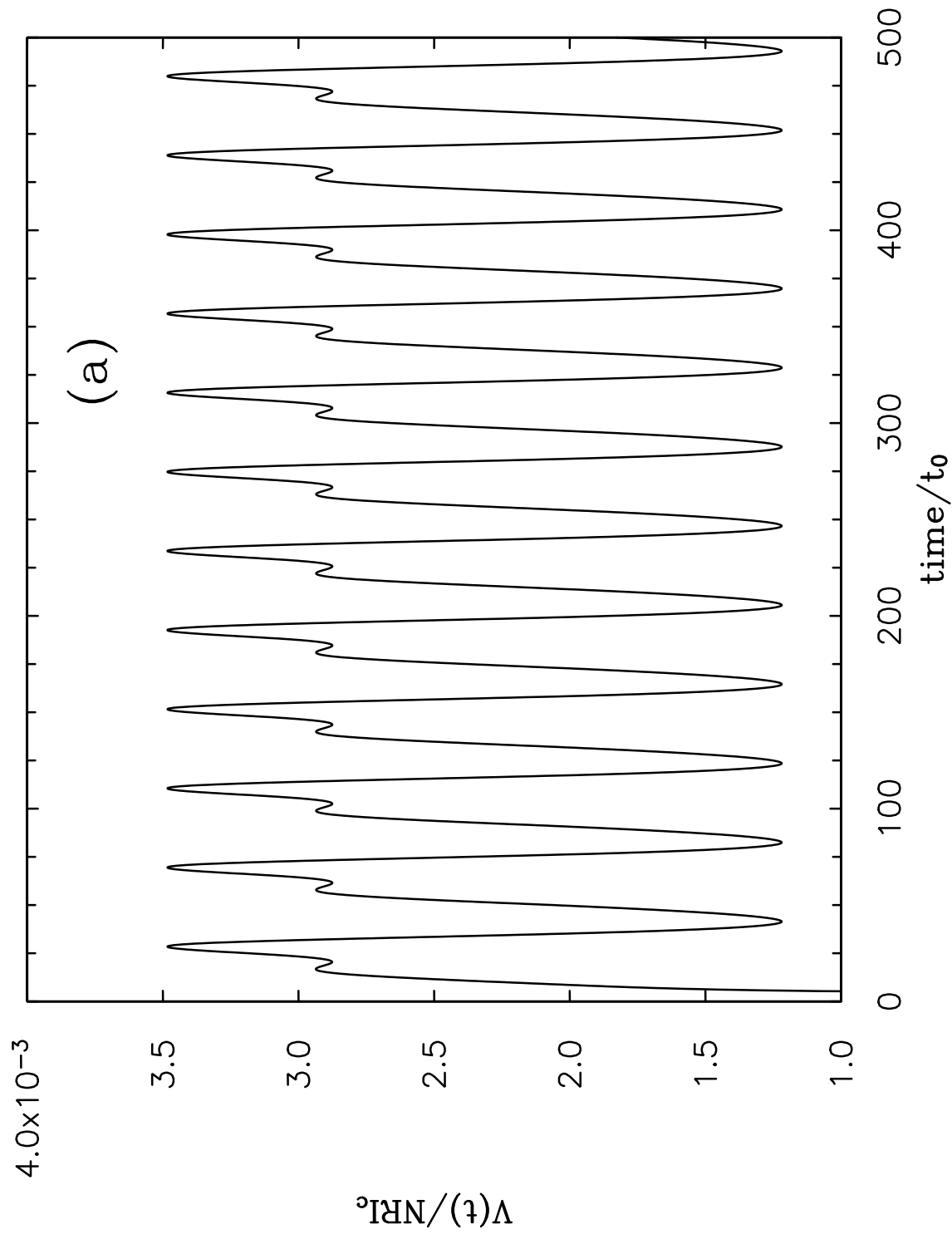


Fig. 5 (a)

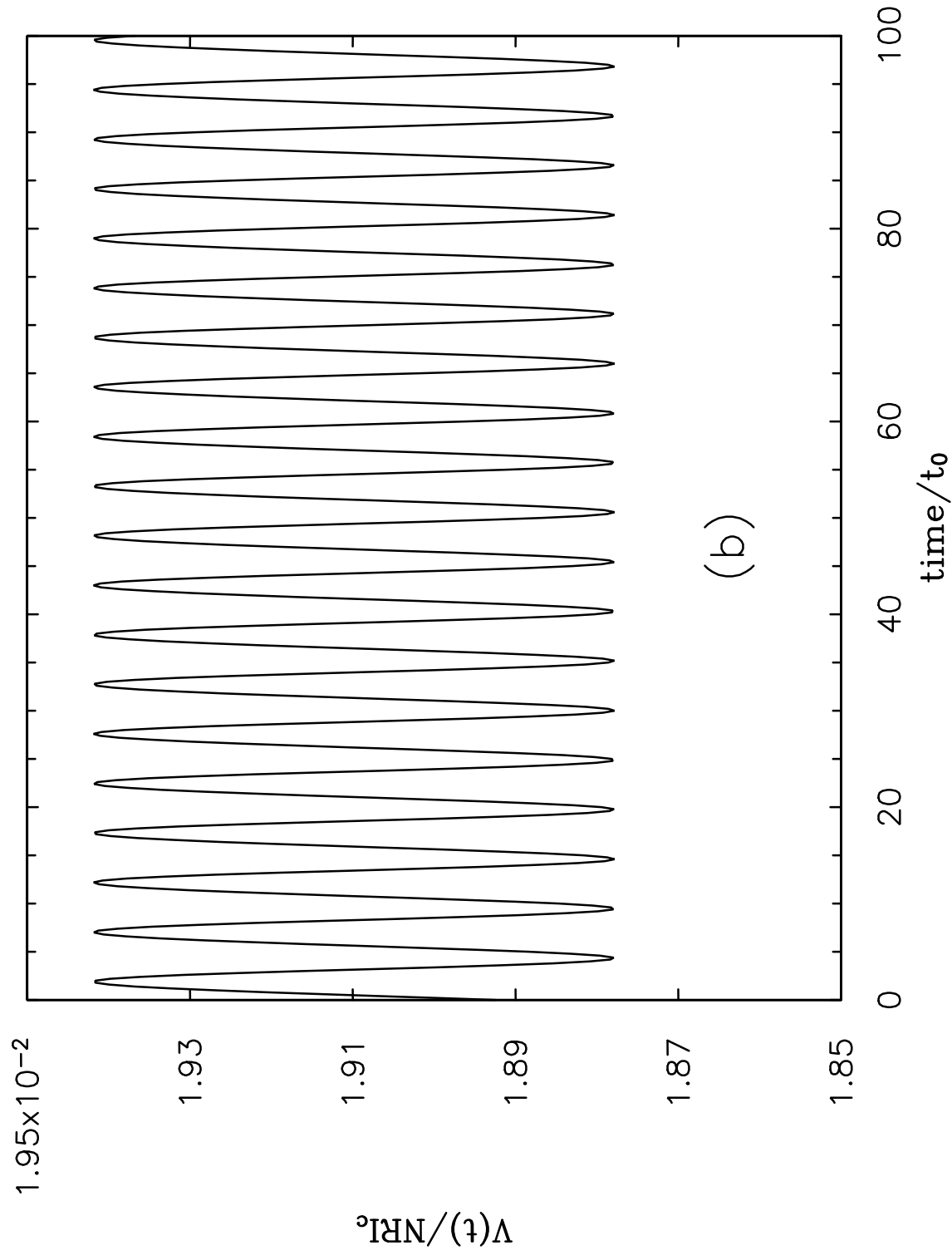
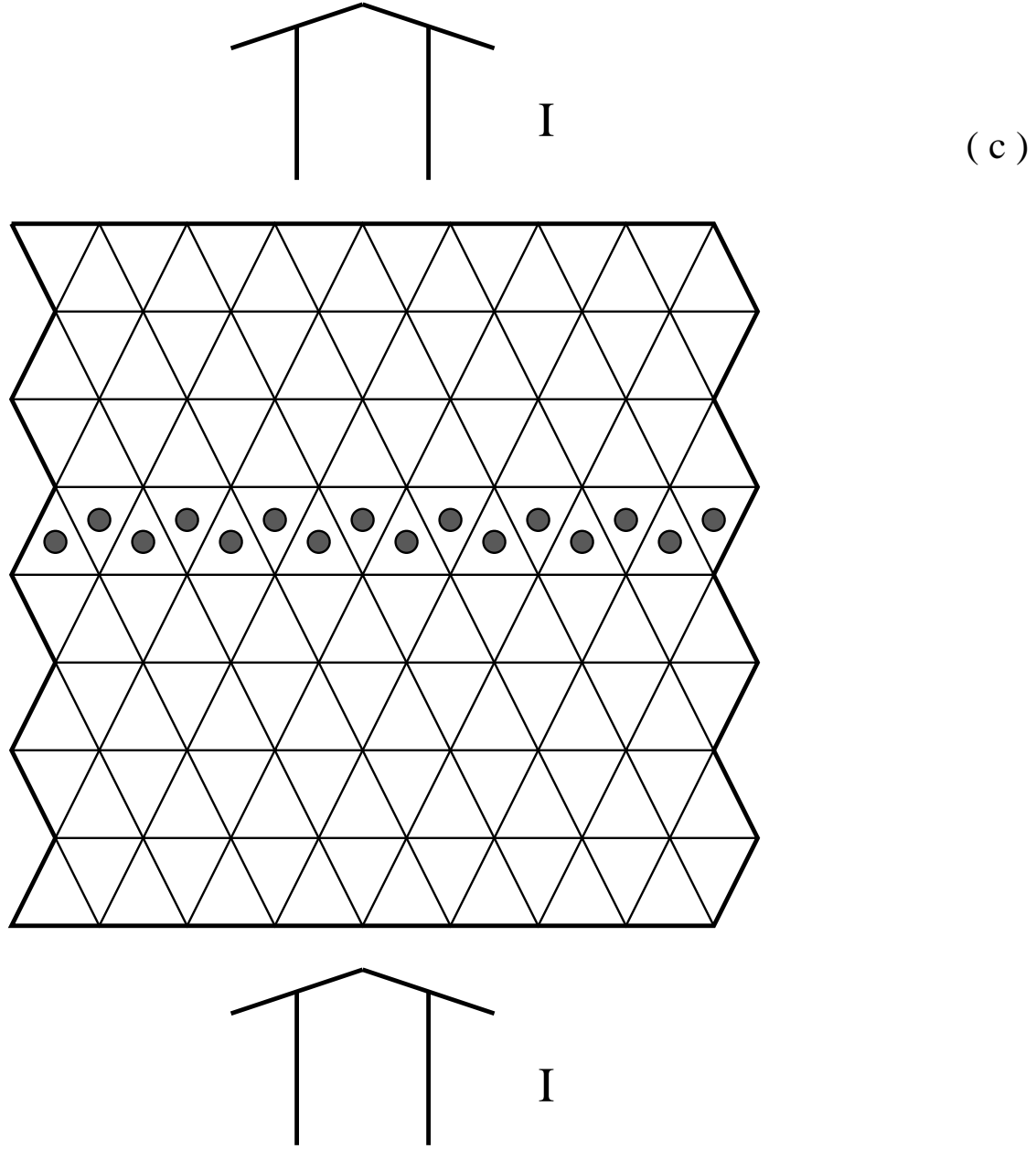


Fig. 5 (b)



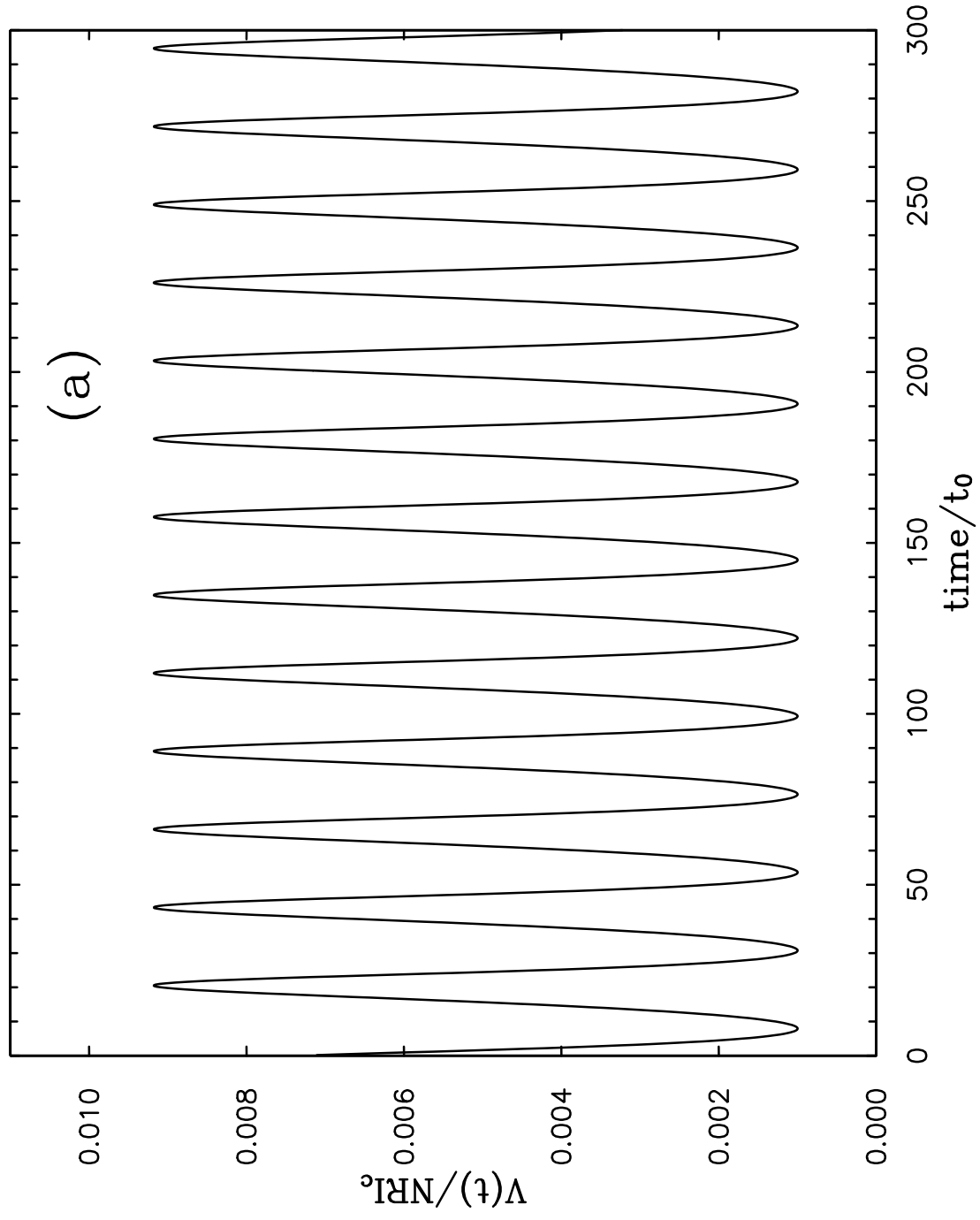


Fig. 6 (a)

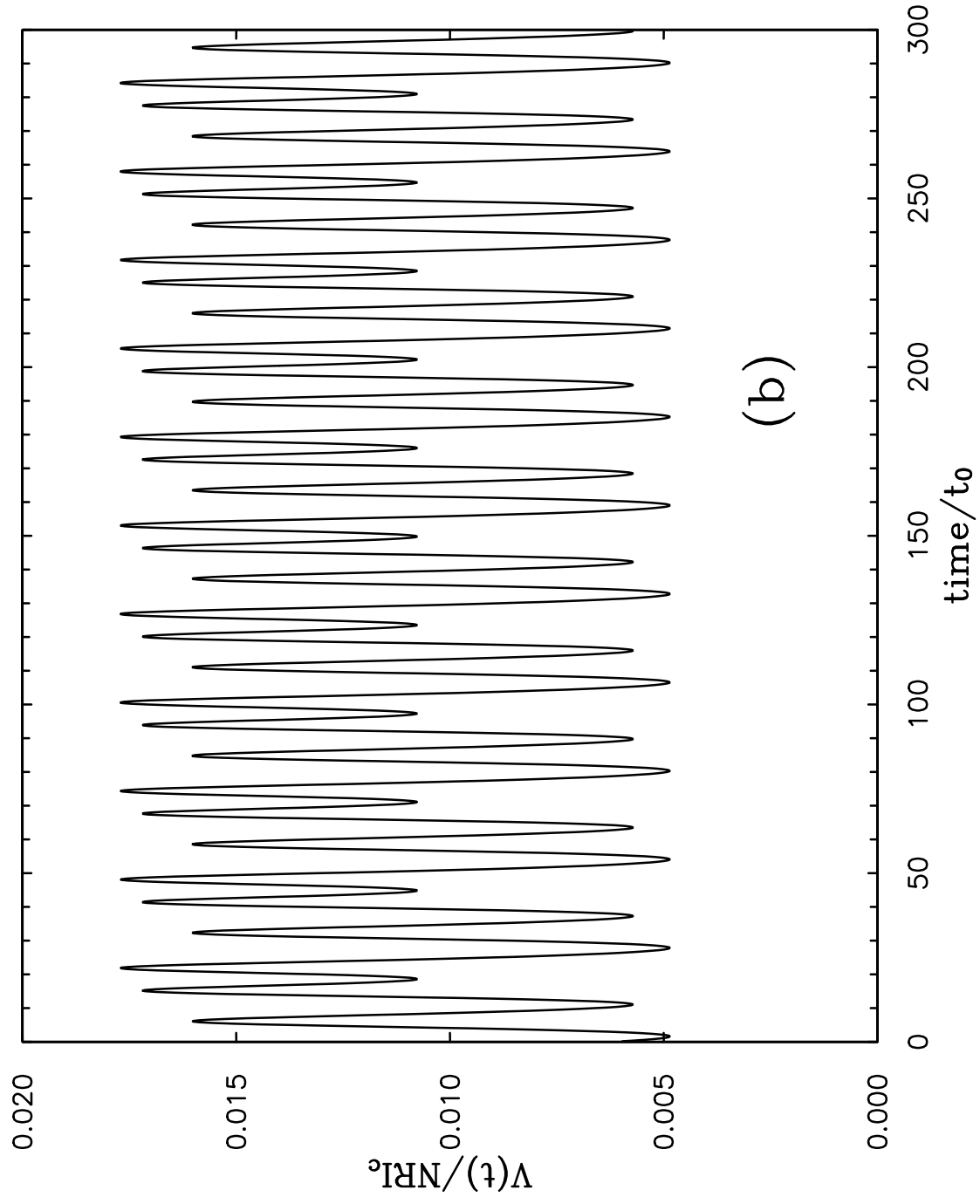


Fig. 6 (b)

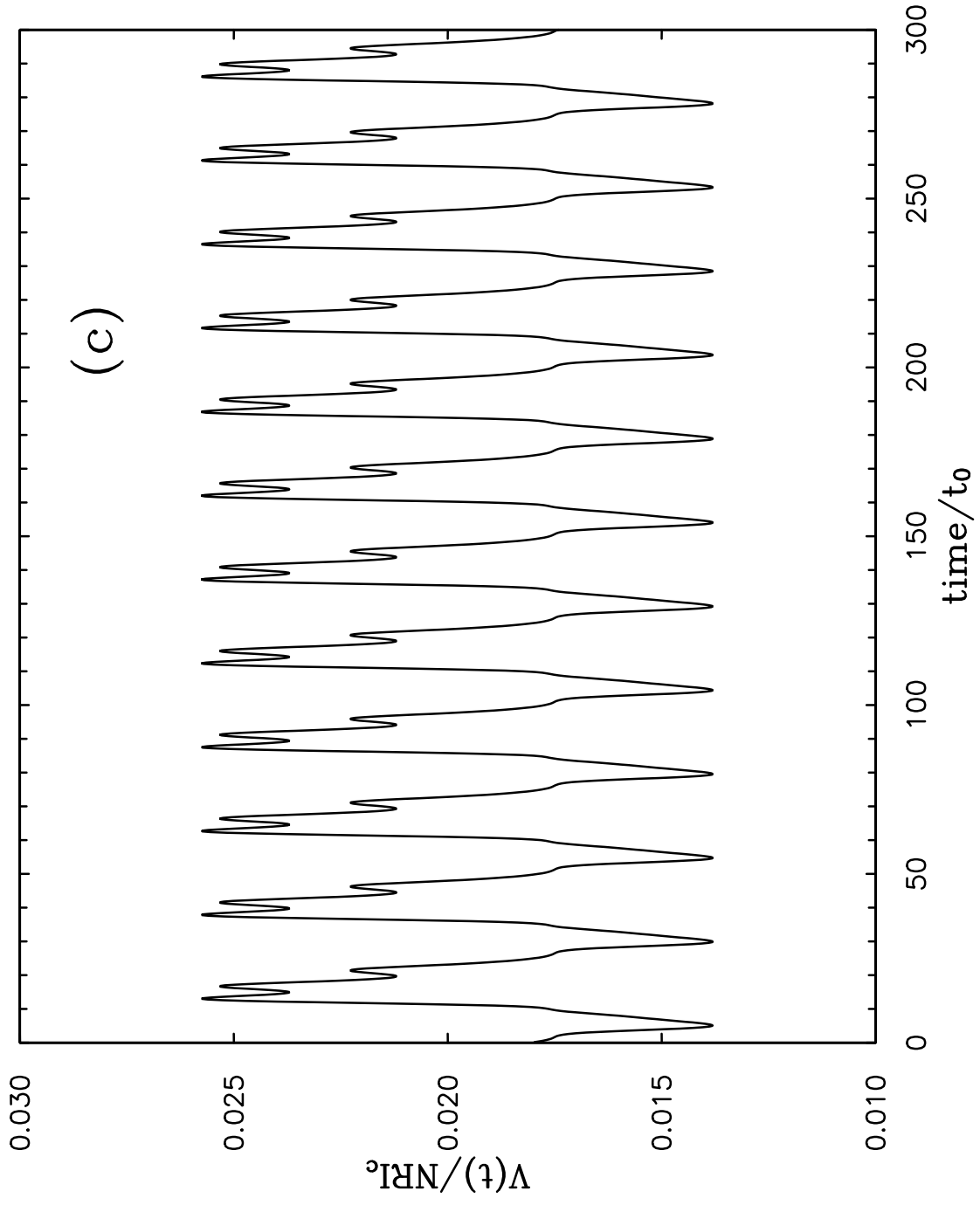
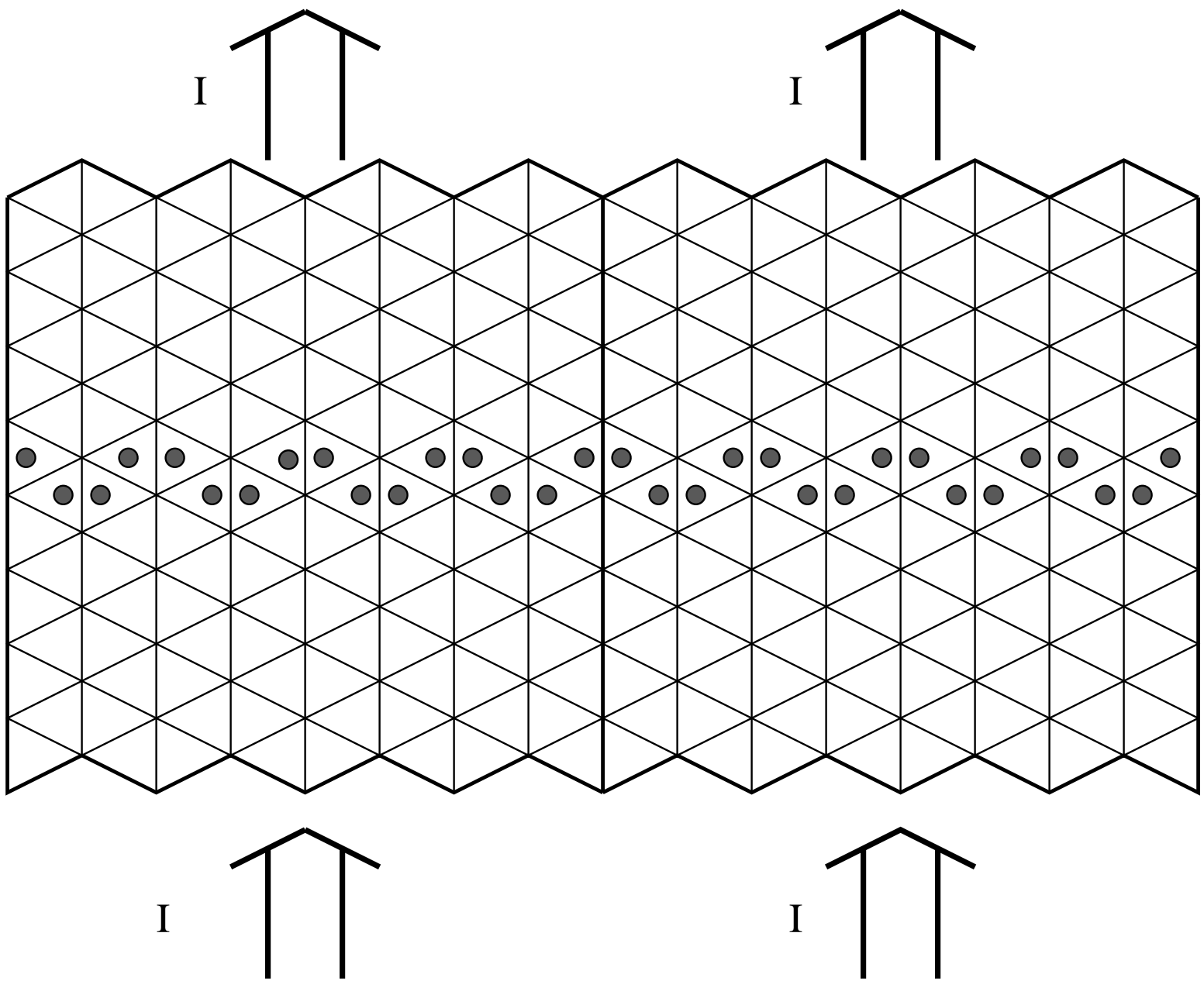
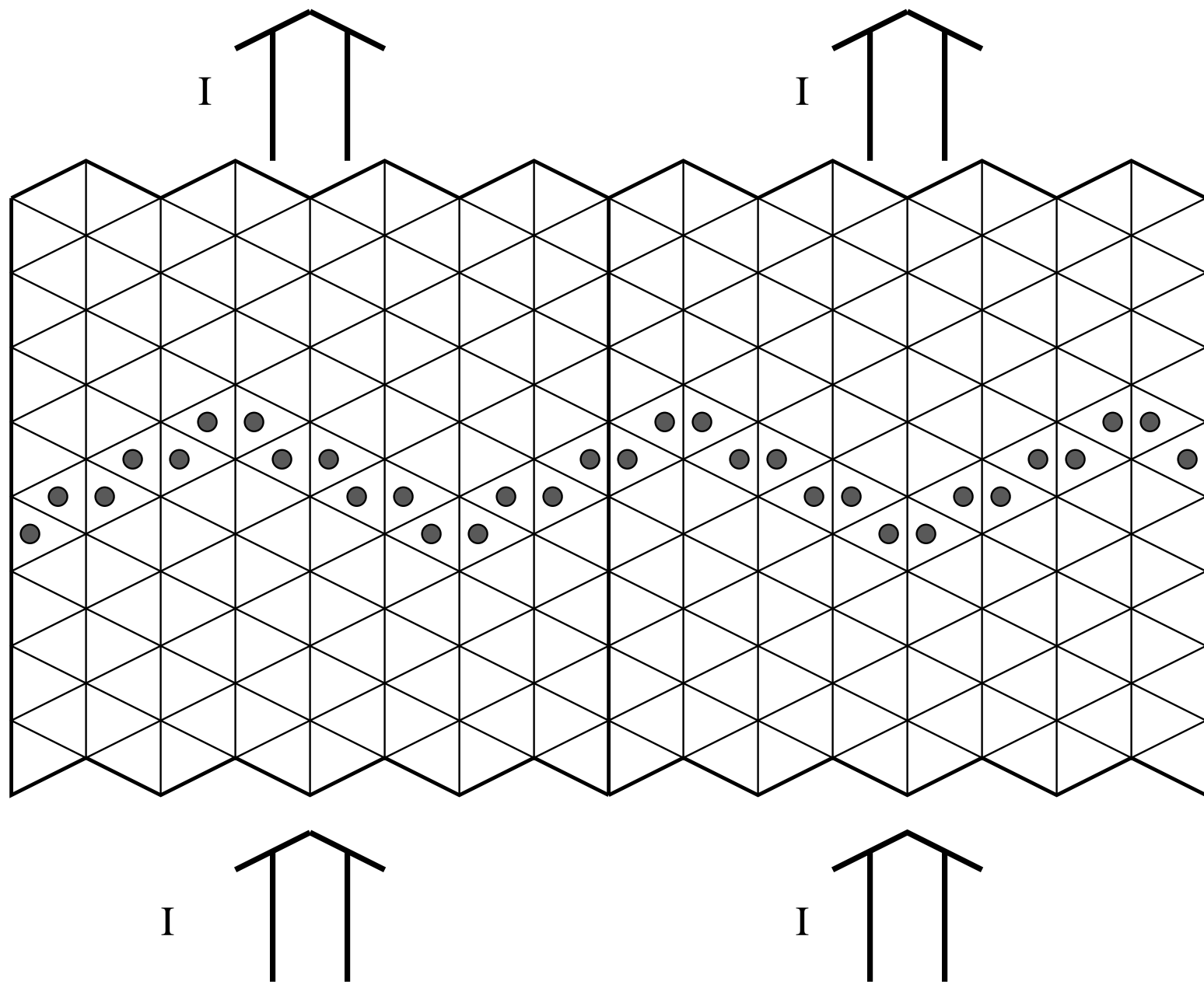


Fig. 6 (c)



(d)



(e)

